Journal of the American Heart Association

ORIGINAL RESEARCH

Protective Effects of Low-Intensity Pulsed Ultrasound on Cardiac Electrophysiological Function in a Rat Model of Ischemic Cardiomyopathy

Zhong-Hao Lin, MD; Qiu-Lu Yu, MD; Bing-Hua Yi, MD; Wen-Cai Xu, MD; Hua-Ling He, MD; Kai-Yu Huang, MD; Cheng Zheng, MD, PhD; Shu-Jie Wu, MD, PhD; Jia-Feng Lin, MD

BACKGROUND: Ischemic cardiomyopathy (ICM) is the end stage of ischemic heart disease, in which ventricular remodeling contributes to a fatal ventricular arrhythmia, worsens heart function and unfavorable outcomes, and is related to persistent chronic inflammation. Low-intensity pulsed ultrasound (LIPUS) is an effective treatment modality for osteoarthropathy and has been illustrated to regulate the overactive inflammatory response in various diseases. Here, we aim to investigate whether LIPUS can perform cardiac protective effects in ICM and explore its possible mechanism.

METHODS: The left anterior descending artery of adult male Sprague–Dawley rats was ligated for 4 weeks to develop ICM and then treated with LIPUS. Vagotomy was applied to suppress the cholinergic anti-inflammatory pathway. Cardiac-specific Cav-1 (caveolin-1) overexpression in ICM on arrhythmias, excitation-contraction coupling, and cardiac remodeling was investigated using the intramyocardial injection of an adeno-associated virus serotype 9 system.

RESULTS: The results showed that LIPUS alleviated ventricular remodeling, improved cardiac electrophysiological function, and reduced the cardiac expression of collagens and inflammatory cytokines. Vagotomy suppressed the improvement of LIPUS. The overexpression of Cav-1 reset the influence of vagotomy.

CONCLUSIONS: We found that LIPUS had a direct effect on regional anti-inflammation and antifibrosis, improved cardiac autonomic function and heart failure, protected the Cx43 (connexin-43) protein, and reduced the risk of malignant arrhythmia during ICM. The cholinergic anti-inflammatory pathway was one of the potential critical mechanisms involved, and Cav-1 might play an important role downstream. Our study provided a new, promising, and noninvasive strategy for treating ICM.

Key Words: caveolin-1 ■ cholinergic anti-inflammatory pathway ■ ischemic cardiomyopathy ■ low-intensity pulsed ultrasound ■ ventricular arrhythmia

Percutaneous artery intervention and other therapies have significantly reduced the mortality and the years of life lost caused by cardiovascular diseases, especially acute myocardial infarction (MI). However, cardiovascular diseases remain a significant cause of disease-related death globally.[1] Ischemic heart disease is the first cause of cardiovascular disease-related death.[2] Patients who survived ischemic heart diseases such as MI may ultimately develop ischemic cardiomyopathy (ICM), with a 5-year survival rate of only 40% to 50%. Ventricular remodeling during ICM contributes to fatal ventricular arrhythmia, worsened

Correspondence to: Jia-Feng Lin, MD and Shu-Jie Wu, MD, PhD, Department of Cardiology, The Second Affiliated Hospital Yuying Children's Hospital of Wenzhou Medical University, Xueyuan West Load 109, Wenzhou, Zhejiang 325027, China. Email: linjiafeng_wzmcfey@163.com and 706872214@qq.com

This article was sent to Kerry-Anne Rye, PhD, Senior Guest Editor, for review by expert referees, editorial decision, and final disposition.

Supplemental Material is available at https://www.ahajournals.org/doi/suppl/10.1161/JAHA.124.037402

For Sources of Funding and Disclosures, see page 12.

JAHA is available at: www.ahajournals.org/journal/jaha

CLINICAL PERSPECTIVE

What Is New?

- We found that regional anti-inflammatory and antifibrotic properties, along with improving cardiac autonomic function, are responsible for the antiarrhythmogenic effects of low-intensity pulsed ultrasound in ischemic cardiomyopathy. The cholinergic anti-inflammatory pathway plays a key role and is related to caveolin-1.

What Are the Clinical Implications?

- Based on our results, mitigating the progression of regional inflammation and fibrosis, along with reducing the sympathetic-to-parasympathetic ratio, may protect against heart failure and fatal ventricular arrhythmias in patients with ischemic cardiomyopathy.
- Low-intensity pulsed ultrasound may be a new, promising, noninvasive treatment strategy for ischemic cardiomyopathy.

Nonstandard Abbreviations and Acronyms

AAV	adeno-associated virus serotype 9
Cav-1	caveolin-1
HF	high-frequency power
ICM	ischemic cardiomyopathy
LF	low-frequency power
LIPUS	low-intensity pulsed ultrasound
LVEDd	left ventricular end-diastolic dimension
LVEDP	left ventricular end-diastolic pressure
LVESd	left ventricular end-systolic dimension
LVSP	left ventricular systolic pressure
RT	return time
SDNN	SD of the averages of normal-to-normal intervals
SDV	sarcomere departure velocity
SRV	sarcomere return velocity
SS	sarcomere shortening
TTP	time to peak

heart function, and unfavorable outcomes, which are related to persistent chronic inflammation.[3]

Researchers first noticed the biological application of focused ultrasonic waves,[4] then tried exploring the influence of frequency and intensity. Now, scientists have done much research about the application of ultrasound in medicine and found low-intensity pulsed ultrasound (LIPUS) to be a potential treatment, especially in fracture healing and old fracture of bone nonunion.[5] Abundant fundamental research and clinical trials show that LIPUS moderates inflammation and immunoreaction in many, including periodontitis,[3] osteoarthrosis,[6] aplastic anemia,[7] and even neurological disorders.[8,9] Some researchers have noticed that LIPUS may be a potential treatment for cardiovascular diseases. Beneficial effects discovered by Shindo et al proved that LIPUS can improve the ventricular remodeling after acute MI, for which mechanotransduction and its downstream pathways may be involved.[10] Recently, it has been demonstrated that LIPUS therapy attenuated the inflammatory response and improved the survival rate of viral myocarditis.[11] Nevertheless, the mechanism behind it remains controversial.

In this study, we aimed to investigate whether the inflammatory modulating effect of LIPUS could act on the harmful, persistent chronic inflammation in ICM and, if so, cast light on the potential mechanisms involved in the beneficial effect.

METHODS

We use the Animal Research: Reporting of In Vivo Experiments reporting guidelines. All animal experiments met the criterion ratified by the Animal Ethics Committee of Wenzhou Medical University (Number wydw2021-0301) and coincided with the *Guide for the Care and Use of Laboratory Animals* issued by the National Institutes of Health. The Cav-1 (caveolin-1) coding sequence is shown in Table S1. The timeline and flow chart of the complete set of experiments are shown in Figure S1. Figure S2 shows the intramyocardial injection and tail vein injection of the adeno-associated virus serotype 9 (AAV9)-cardiac troponin T system. Data S1 describes detailed reagent information, animal preparation and treatment, and experimental methods. The data are expressed as the means±SD. The data, analytical techniques, and study materials are available from the corresponding author and first author upon reasonable request.

Statistical Analysis

SPSS software (Unicom, Mosson Hills, CA, USA) was used for statistical analyses. For data with variance homogeneity, all outcomes among groups were compared using a 1-way ANOVA, followed by the Dunnett multiple-comparison test. Kruskal-Wallis H test was used on the ranked data of inducibility of ventricular arrhythmias induced by programmed electrical sitmulation.

RESULTS

Effect of LIPUS on Cardiac Ejection Function

In Figure 1, echocardiography was used to measure the cardiac function of all the rats before and after the

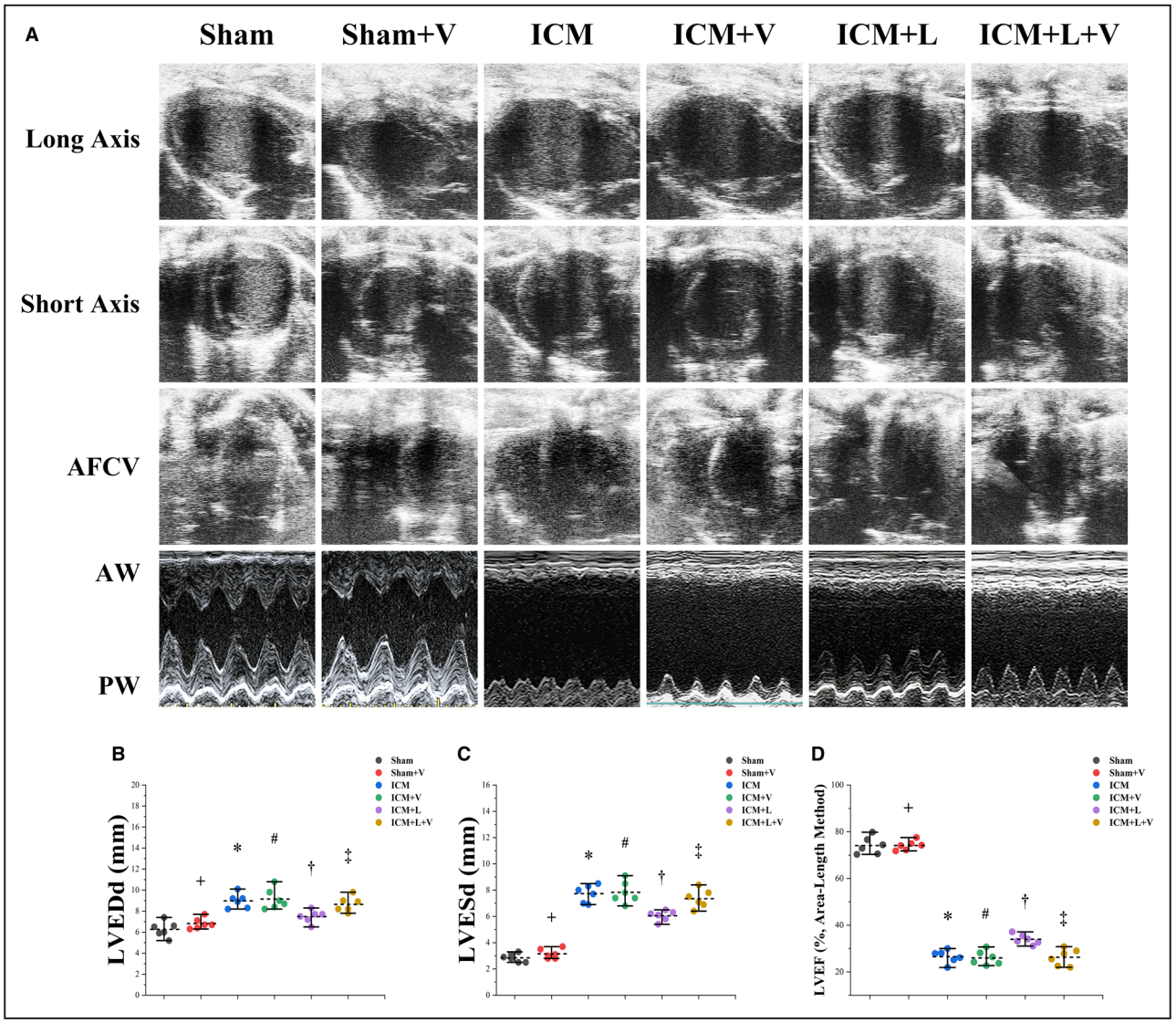

Figure 1. Effect of LIPUS on the cardiac ejection function.
A, The M-mode and B-mode echocardiogram views of Sham-operated rats (Sham, n=6), vagotomy rats (Sham+V, n=6), 8 weeks after left anterior descending coronary artery ligation rats (ICM, n=6), ICM rats received vagotomy (ICM+V, n=6), 4-week LIPUS treatment after 4-week left anterior descending coronary artery ligation rats (ICM+L, n=6), ICM rats with vagotomy and 4-week LIPUS treatment (ICM+L+V, n=6). **B** through **D**, The difference of LVEDd, LVESd, and area-length method LVEF among Sham group, Sham+V group, ICM group, ICM+V group, ICM+L group and ICM+L+V group. The AW of ICM rats performed distinct akinesis and the PW showed a certain degree of hypomotility, and the left ventricular cavity expanded significantly. Compared with ICM group, LIPUS treatment reduced the LVEDd, LVESd, improved LVEF. LVEDd, LVESd, and LVEF were similar between the ICM group and ICM+L+V group. All the data are expressed as the means±SD, $^{*}P<0.05$ compared with Sham group, $^{\dagger}P<0.05$ compared with ICM group, $^{\ddagger}P<0.05$ compared with ICM+L group, $^{+}P>0.05$ compared with Sham group, $^{\#}P>0.05$ compared with ICM group. The actual *P* values can be found in the Results. AFCV indicates apical 4-chamber view; AW, anterior wall; ICM, ischemic cardiomyopathy; L, LIPUS group; LIPUS, low-intensity pulsed ultrasound; LVEDd, left ventricular end-diastolic dimension; LVEF, left ventricular ejection fraction; LVESd left ventricular end-systolic dimension; PW, posterior wall; and V, vagotomy group.

experiments. The ICM group had higher left ventricular end-diastolic dimension (LVEDd; 6.27±0.75 versus 8.98±0.70, *P*=0.001), left ventricular end-systolic dimension (LVESd; 2.85±0.32 versus 7.73±0.67, *P*<0.001), and lower left ventricular ejection fractions (area-length method LVEF; 74.11±3.67 versus 26.52±2.82, *P*<0.001) than the Sham group. The 4-week LIPUS improved these indicators (ICM+LIPUS versus ICM, LVEDd 7.48±0.60 versus 8.98±0.70, *P*=0.032; LVESd 6.05±0.39 versus 7.73±0.67, *P*=0.008; area-length method LVEF 33.96±2.16 versus 26.52±2.82, *P*=0.007). The LVEDd, LVESd, and LVEF of the ICM+LIPUS+vagotomy group were significantly

weaker when compared with the ICM+LIPUS group (ICM+LIPUS+vagotomy versus ICM+LIPUS, LVEDd 8.65±0.73 versus 7.48±0.60, *P*=0.009; LVESd 7.35±0.71 versus 6.05±0.39, *P*=0.049; area-length method LVEF 26.28±3.56 versus 33.96±2.16, *P*=0.021). Vagotomy did not show a significant difference in the Sham+vagotomy group (Sham versus Sham+vagotomy, LVEDd *P*=0.849, LVESd *P*=0.847, area-length method LVEF *P*=1.000) and the ICM+vagotomy group (ICM versus ICM+vagotomy, all *P*=1.000).

Effect of LIPUS on Fibrosis and Inflammatory Cytokine Production of the Infarct Border Zone

In Figure 2, Masson's trichrome staining was applied to show the area of fibrosis in the infarct border zone. The Western blotting displayed collagen synthesis/release and proinflammatory cytokine production. Compared with the Sham group, the fibrosis area of the ICM group was significantly increased (fibrosis area %, Sham versus ICM, 0.04±0.01 versus 0.50±0.02, *P*<0.001), as was the synthesis/release of collagen and proinflammatory cytokine production (Sham versus ICM, collagen I 0.05±0.01 versus 0.95±0.13, *P*<0.001; collagen III 0.08±0.01 versus 1.33±0.28, *P*=0.001; p-NF-κB (phospho-nuclear factor kappa B) p65/NF-κB p65 0.02±0.00 versus 1.21±0.15, *P*<0.001; TNFα (tumor necrosis factor alpha) 0.06±0.00 versus 1.64±0.23, *P*<0.001; IL-6 (interleukin-6) 0.06±0.01 versus 1.27±0.29, *P*=0.002; IFN-γ (interferon gamma) 0.03±0.01 versus 1.42±0.29, *P*=0.002). LIPUS improved collagen synthesis/release, decreased proinflammatory cytokine production, and lessened the dilation of the fibrosis area (ICM+LIPUS group; fibrosis area % 0.43±0.03 *P*=0.018, collagen I 0.37±0.08 *P*<0.001, collagen III 0.43±0.14 *P*=0.003, p-NF-κB p65/NF-κB p65 0.40±0.05 *P*<0.001, TNFα 0.57±0.07 *P*<0.001, IL-6 0.55±0.11 *P*=0.011, IFN-γ 0.64±0.09 *P*=0.018; all compared with the ICM group). Vagotomy inhibited

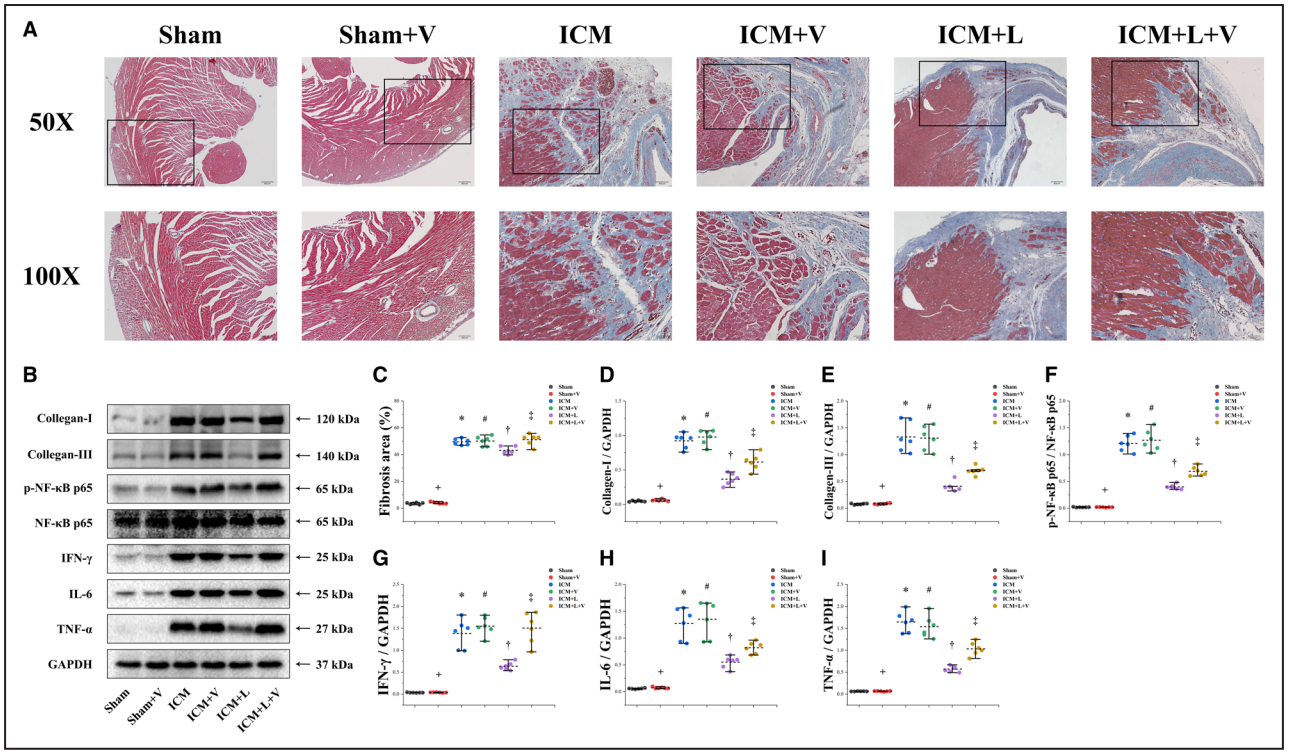

Figure 2. Effect of LIPUS on fibrosis and inflammatory cytokines production of infarct border zone.
A, Fibrosis area of border zone (%) among 6 groups (Sham group, n=6; Sham+V group, n=6; ICM group, n=6; ICM+V group, n=6; ICM+L group, n=6; ICM+L+V group, n=6; upper magnification ×50; lower magnification ×100). **B**, the Western blotting results, n=6 for each group. **C** through **I**, analysis results of (**A**) and (**B**). Compared with Sham group, fibrosis in the infarct border zone, collagen synthesis/release and inflammatory response were significantly increased in ICM group. LIPUS treatment showed an evident improvement of these targets. The vagotomy attenuated these effects of LIPUS treatment. All data are expressed as the means±SD. **P*<0.05 compared with Sham group, †*P*<0.05 compared with ICM group, ‡*P*<0.05 compared with ICM+L group, +*P*>0.05 compared with Sham group, #*P*>0.05 compared with ICM group. The actual *P* values can be found in the Results. ICM indicates ischemic cardiomyopathy; IFN-γ, interferon gamma; IL-6, interleukin 6; L, LIPUS group; LIPUS, low-intensity pulsed ultrasound; NF-κB, nuclear factor kappa B; p-NF-κB, phospho-nuclear factor kappa B; TNFα, tumor necrosis factor alpha; and V, vagotomy group.

the modified effects of LIPUS (ICM+LIPUS+vagotomy group; fibrosis area % 0.51±0.04 *P*=0.046, collagen I 0.62±0.12 *P*=0.027, collagen III 0.70±0.08 *P*=0.002, p-NF-κB p65/NF-κB p65 0.69±0.09 *P*=0.001, TNFα 1.03±0.15 *P*=0.003, IL-6 0.82±0.11 *P*=0.022, IFN-γ 1.51±0.36 *P*=0.014; all compared with the ICM+LIPUS group). Alternatively, vagotomy intervention in the Sham and ICM rats did not show meaningful results (Sham versus Sham+vagotomy, fibrosis area % *P*=0.958, collagen I *P*=0.516, collagen III *P*=1.000, p-NF-κB p65/NF-κB p65 *P*=1.000, TNFα *P*=1.000, IL-6 *P*=0.744, IFN-γ *P*=0.991; ICM versus ICM+vagotomy, fibrosis area % *P*=1.000, collagen I *P*v0.997, collagen III *P*=1.000, p-NF-κB p65/NF-κB p65 *P*=1.000, TNFα *P*=0.999, IL-6 *P*=1.000, IFN-γ *P*=0.981).

Effect of LIPUS on Cardiac Autonomic Nerve Function and Programmed Electric Stimulation-Induced Malignant Arrhythmia

Cardiac autonomic function was evaluated by the time domain and frequency domain of heart rate variability, indicated with SD of the averages of normal-to-normal intervals (SDNN) and low-frequency power/high-frequency power (LF/HF) ratio (Figure 3). The Sham

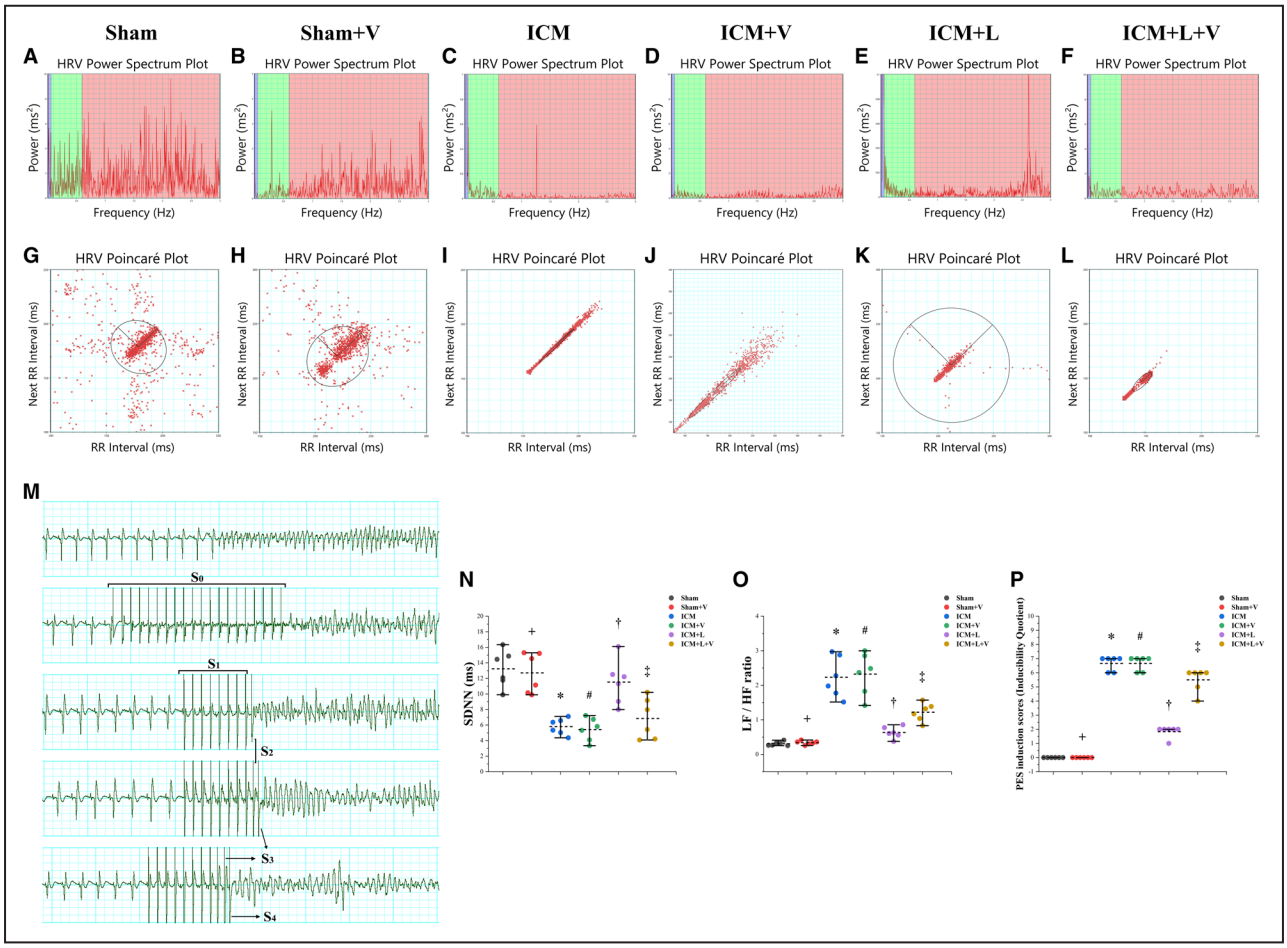

Figure 3. Effect of LIPUS on cardiac autonomic nerve function and on PES-induced malignant arrhythmia.
A through **F**, LF/HF ratio of HRV obtained from 6 groups; **G** through **L**, Time domain parameter of HRV obtained from 6 groups, SDNN (**A** and **G**: Sham group; **B** and **H**: Sham+V group; **C** and **I**: ICM group; **D** and **J**: ICM+V group; **E** and **K**: ICM+L group; **F** and **L**: ICM+L+V group; all n=8). **M**, the schematic diagram of ventricular PES: S_0, burst, 20 pace beats at 100 milliseconds; S_1, 8 paced beats at a basic cycle length of 100 milliseconds; S_2, S_3, and S_4 represent extra stimuli. **N** and **O**, Compared with Sham group, ICM group showed a significant decrease in SDNN and a significant increase in LF/HF ratio. LIPUS treatment increased the SDNN and decreased the LF/HF ratio of ICM rats. Vagotomy operation attenuated the effect of LIPUS treatment. **P**, PES induction scores, inducibility quotient of ventricular arrhythmias. All data are expressed as the means±SD. Kruskal–Wallis H test was used to test the ranked data of inducibility of ventricular arrhythmias induced by PES. **P*<0.05 compared with Sham group, †*P*<0.05 compared with ICM group, ‡*P*<0.05 compared with ICM+L group, ⁺*P*>0.05 compared with Sham group, #*P*>0.05 compared with ICM group. The actual *P*-values can be found in the Results. HRV indicates heart rate variability; ICM, ischemic cardiomyopathy; L, LIPUS group; LF/HF low-frequency power/high-frequency power; LIPUS, low-intensity pulsed ultrasound; PES, programmed electric stimulation; SDNN, SD of the averages of normal-to-normal intervals; and V, vagotomy group.

Table 1. Effect of LIPUS on ECG Data

Group	RR (msec)	PR (msec)	*P* (msec)	QRS (msec)	QTc (msec)
Sham	196.90±20.49	50.61±0.94	17.59±1.31	25.59±2.34	133.82±3.23
Sham+vagotomy	192.33±18.75	50.71±1.06	17.95±1.57	25.87±3.17	134.41±4.50
ICM	193.77±20.22	50.24±1.59	18.07±1.35	25.91±1.83	171.56±6.71*
ICM+vagotomy	196.78±19.02	50.55±3.20	17.81±1.61	25.65±2.84	173.87±9.30
ICM+LIPUS	194.92±17.98	50.82±2.23	18.21±1.26	25.24±1.88	153.45±8.26†
ICM+LIPUS+vagotomy	197.97±24.12	50.80±3.15	18.04±2.12	25.82±3.63	164.33±9.47‡

n=8 of each group. ICM indicates ischemic cardiomyopathy; LIPUS, low-intensity pulsed ultrasound; P, P-wave duration; PR, P-R interval; QRS, QRS-wave interval; QTc, heart rate-corrected QT interval; and RR, R-R interval. Data are presented as means±SD.

*P<0.05 compared with Sham group.

†P<0.05 compared with ICM group.

‡P<0.05 compared with ICM+LIPUS group. The actual P values can be found in the Results.

group and Sham+vagotomy group, the ICM group, and the ICM+vagotomy group had similar SDNN and LF/HF ratios (Sham versus Sham+vagotomy, SDNN 13.05±2.77 versus 13.84±3.09 P=1.000, LF/HF 0.30±0.07 versus 0.31±0.07 P=1.000; ICM versus ICM+vagotomy, SDNN 5.63±0.94 versus 5.91±1.55 P=1.000, LF/HF 2.11±0.64 versus 2.11±0.70 P=1.000). Compared with the Sham group, the ICM group showed a significant decrease in SDNN (P=0.001) and an increase in the LF/HF ratio (P=0.001). LIPUS increased SDNN and decreased LF/HF ratios in the ICM rats (ICM+LIPUS group, SDNN 11.75±2.62 P=0.002, LF/HF 0.65±0.15 P=0.003, versus ICM group), and vagotomy in the ICM+LIPUS group negatively affected SDNN and LF/HF ratios (ICM+LIPUS+vagotomy group; SDNN 7.09±2.39 P=0.03, LF/HF 1.15±0.26 P=0.007, versus ICM+LIPUS group). On the other hand, programmed electric stimulation-induced malignant arrhythmia showed ICM rats had higher ventricular arrhythmia quotients (ICM versus Sham, P<0.001), and LIPUS-treated rats showed lower quotients (ICM+LIPUS versus ICM, 2.13±0.64 versus 6.75±0.46, P<0.001). Vagotomy induced the positive effects of LIPUS (ICM+LIPUS+vagotomy versus ICM+LIPUS, 5.88±0.99 versus 2.13±0.64, P<0.001), but in the Sham group and ICM group, vagotomy did not show significant differences (Sham versus Sham+vagotomy, P=1.000; ICM versus ICM+vagotomy, 6.75±0.46 versus 6.88±0.64, P=1.000).

Effect of LIPUS on ECG Data and Left Ventricular Pressure

Tables 1 and 2 provide further proof of the positive effects of LIPUS. The ICM group displayed prolonged QTc (ICM versus Sham, P<0.001). The LIPUS improved QTc (ICM+LIPUS versus ICM, P<0.001), and vagotomy reduced this positive effect (ICM+LIPUS+vagotomy versus ICM+LIPUS, P<0.001). The RR interval, PR interval, P-wave duration, and duration of QRS in each group were similar (P>0.05). The QTc did not show significant differences in the Sham or ICM groups after vagotomy (Sham versus Sham+vagotomy P=1.000, ICM versus ICM+vagotomy P=0.875). Higher systolic blood pressure (SBP), diastolic blood pressure, and left ventricular systolic pressure (LVSP) and lower left ventricular end-diastolic pressure (LVEDP) indicated enhanced cardiac function. The ICM group displayed lower SBP, diastolic blood pressure, and LVSP and higher LVEDP than the Sham group (ICM versus Sham, all P<0.001). Compared with the ICM group, LIPUS improved SBP, LVSP, and LVEDP (ICM+LIPUS versus ICM, all P<0.001). The ICM+LIPUS+vagotomy group showed lower SBP, diastolic blood pressure,

Table 2. Effect of LIPUS on Left Ventricular Pressure

Group	HR (bpm)	SBP (mm Hg)	DBP (mm Hg)	LVSP (mm Hg)	LVEDP (mm Hg)
Sham	359±11	100.83±2.80	73.72±3.12	136.89±2.29	2.64±0.54
Sham+vagotomy	359±13	100.56±2.97	74.28±2.78	136.50±2.12	2.69±0.52
ICM	351±19	87.42±3.56*	63.50±3.27*	92.64±2.66*	7.64±1.07*
ICM+vagotomy	352±19	86.83±3.36	63.42±3.48	92.50±2.51	7.61±0.93
ICM+LIPUS	358±21	93.06±3.81†	68.11±2.88†	109.97±3.87†	4.75±0.97†
ICM+LIPUS+vagotomy	355±20	88.53±3.86‡	65.03±2.61‡	100.11±3.97‡	6.22±1.02‡

n=6 of each group. DBP indicates diastolic blood pressure; HR, heart rate; ICM, ischemic cardiomyopathy; LIPUS, low-intensity pulsed ultrasound; LVSP, left ventricular systolic pressure; LVEDP, left ventricular end-diastolic pressure; and SBP, systolic blood pressure. All the data are present as means±SD. The actual P values can be found in the Results.

*P<0.05 compared with Sham group.

†P<0.05 compared with ICM group.

‡P<0.05 compared with ICM+LIPUS group.

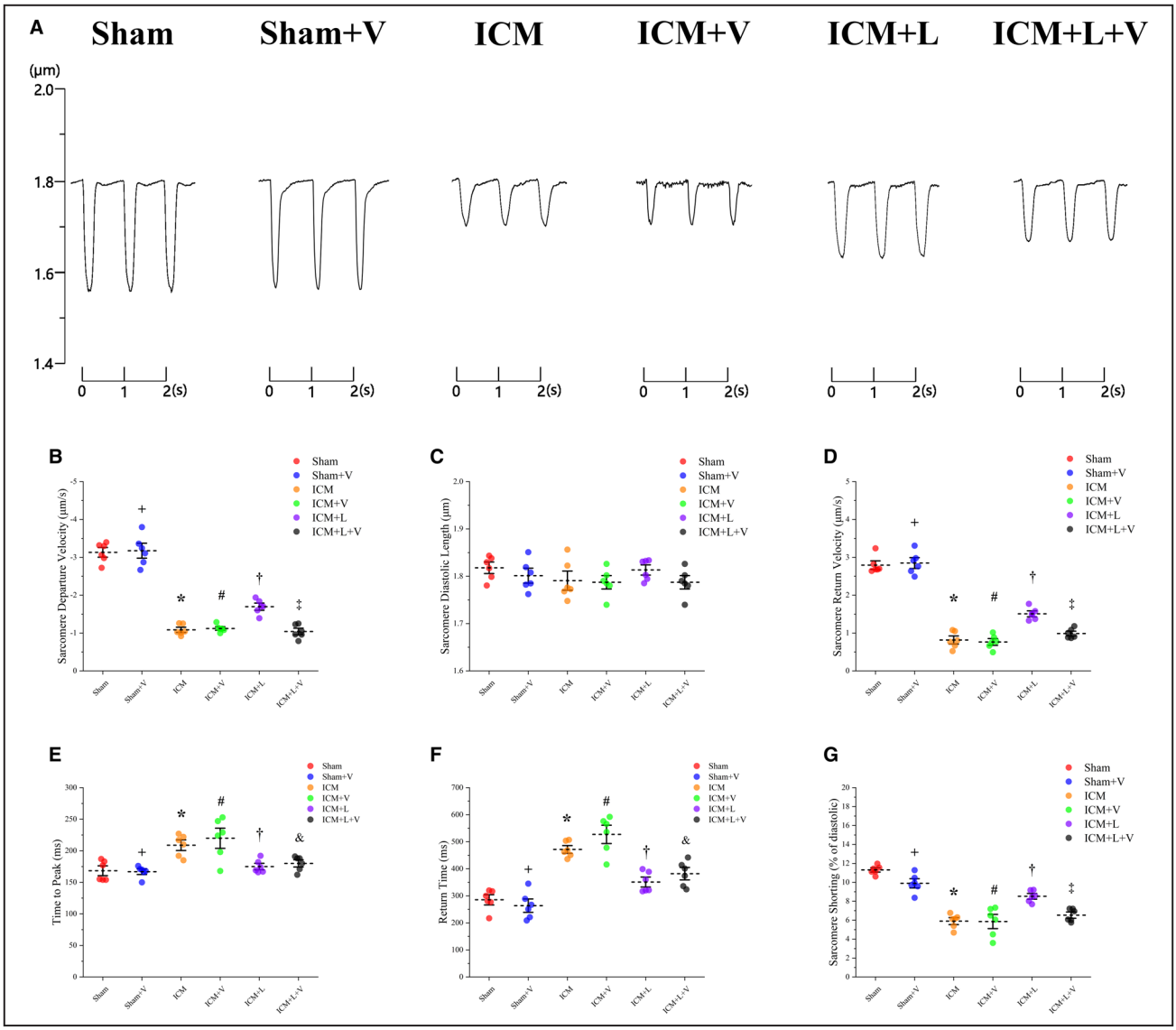

Figure 4. Effect of LIPUS on sarcomere contraction measurement.

A, Typical single-myocyte sarcomere-contraction original trace of each group. **B** through **G**, Data of sarcomere contraction of each group. No significant differences were found in sarcomere diastolic length among 6 groups. The ICM group had lower SS, lower SDV, lower SRV, longer TTP and longer RT than the Sham group. Higher SS, SDV, and SRV and shorter TTP and RT were found in the ICM+L group when compared with ICM group. Vagotomy decreased SS, SDV and SRV in the ICM+L+V group. There were no differences between the Sham group and the Sham+V group. All the data are expressed as the means±SD. $^{*}P<0.05$ compared with Sham group, $^{\dagger}P<0.05$ compared with ICM group, $^{\ddagger}P<0.05$ compared with ICM+L group, $^{+}P>0.05$ compared with Sham group, $^{\#}P>0.05$ compared with ICM group, $^{\&}P>0.05$ compared with ICM+L group. The actual *P*-values can be found in the Results. ICM indicates ischemic cardiomyopathy; L, LIPUS group; LIPUS, low-intensity pulsed ultrasound; RT, return time; SDV, sarcomere departure velocity; SRV, sarcomere return velocity; SS, sarcomere shortening; TTP, time to peak; and V, vagotomy group.

and LVSP and higher LVEDP (ICM+LIPUS+vagotomy versus ICM+LIPUS, all $P<0.001$).

Effect of LIPUS on Sarcomere Contraction Measurement

Single-myocyte sarcomere fractional shortening was evaluated by sarcomere length during resting state and at 1 Hz, 1 milliseconds, 15 V stimulation under steady state (Figure 4). Figure 4A shows the single-myocyte sarcomere contraction original traces of each group representatively. No significant differences were found in sarcomere diastolic length among the 6 groups. The ICM group rats had significantly lower sarcomere shortening (SS), lower sarcomere departure velocity (SDV), lower sarcomere return velocity (SRV) and longer time to peak (TTP) and longer return time (RT) than the Sham group (Sham group versus the ICM group; SS 11.31±0.46 versus 5.90±0.74 $P<0.001$, SDV −3.13±0.26 versus −1.08±0.14

P<0.001, SRV 2.79±0.23 versus 0.82±0.22 *P*<0.001, TTP 168.33±15.67 versus 208.83±16.87 *P*=0.019, RT 285.33±37.89 versus 471.67±28.55 *P*<0.001). Compared with the ICM group, the ICM+LIPUS group had higher SS, SDV, and SRV and shorter TTP and RT (ICM versus ICM+LIPUS; SS 5.90±0.74 versus 8.52±0.61 *P*=0.001, SDV –1.08±0.14 versus –1.70±0.19 *P*=0.002, SRV 0.82±0.22 versus 1.51±0.16 *P*=0.002, TTP 208.83±16.87 versus 175.00±10.20 *P*=0.032, RT 471.67±28.55 versus 351.00±37.00 *P*=0.001). Vagotomy decreased SS, SDV, and SRV (ICM+LIPUS versus ICM+LIPUS+vagotomy; SS 8.52±0.61 versus 6.53±0.66 *P*=0.004, SDV –1.70±0.19 versus –1.04±0.18 *P*=0.001, SRV 1.51±0.16 versus 0.99±0.13 *P*=0.001), but there were no significant differences between the Sham group and Sham+vagotomy group (Sham+vagotomy, SS 9.89±0.97 *P*=0.135, SDV –3.18±0.39 *P*=1.000, SRV 2.85±0.29 *P*=1.000, TTP 166.72±8.73 *P*=1.000, RT 263.68±49.57 *P*=0.997, all compared with Sham group), ICM group and ICM+vagotomy group (ICM+vagotomy, SS 5.86±1.50 *P*=1.000, SDV –1.12±0.10 *P*=1.000, SRV 0.76±0.18 *P*=1.000, TTP 219.76±31.96 *P*=0.999, all compared with ICM group).

Effect of LIPUS on Alpha-7 Nicotinic Receptor, Cav-1, and Connexin 43 Distribution

In Figure 5, the Western blotting and immunofluorescence assay showed that the expression of protein Cx43 (connexin-43) was significantly decreased in the ICM rats when compared with the Sham rats, and compared with the Sham group (ICM versus Sham, Cx43/GADPH 0.12±0.04 versus 0.98±0.32, *P*<0.001), F-actin was increased and nonuniform in the ICM group. The intervention of LIPUS improved the expression of Cx43 (ICM versus ICM+LIPUS, Cx43/GADPH 0.12±0.04 versus 0.49±0.13, *P*=0.002). Vagotomy downregulated the effect of LIPUS intervention (ICM+LIPUS+vagotomy versus ICM+LIPUS, 0.24±0.05 versus 0.49±0.13, *P*=0.014). The Western blotting results showed that alpha-7 nicotinic receptor (α7-nAChR) was lower in the ICM group (compared with Sham group) and ICM+LIPUS+vagotomy group (compared with ICM+LIPUS group) and higher in the ICM+LIPUS group (compared with ICM group). The Western blotting results of protein Cav-1 also was lower in the ICM group (compared with Sham group) and ICM+LIPUS+vagotomy group (compared with ICM+LIPUS group), and higher in the ICM+LIPUS group (compared with ICM group). (ICM versus Sham, α7-nAChR/GAPDH 0.49±0.10 versus 0.95±0.10, *P*<0.001; Cav-1/GAPDH 0.26±0.05 versus 0.40±0.03, *P*<0.001; ICM versus ICM+LIPUS, α7-nAChR/GAPDH 0.49±0.10 versus 0.68±0.07, *P*=0.04; Cav-1/GAPDH 0.26±0.05 versus 0.35±0.04, *P*=0.04; ICM+LIPUS+vagotomy versus ICM+LIPUS, α7-nAChR/GAPDH 0.42±0.07 versus 0.68±0.07, *P*=0.001; Cav-1/GAPDH 0.24±0.05 versus 0.35±0.04, *P*=0.001).

Cav-1 Overexpression Reversed the Negative Influences of Vagotomy on LIPUS

In Figure 6A, the coimmunoprecipitation experiments were performed to determine the underlying mechanism of the favorable properties of LIPUS in ICM rats. Immunoprecipitation with α7-nAChR, Cav-1, cSRC, and normal rabbit immunoglobulin G; Cav-1, cSRC, Cx43, and normal rabbit immunoglobulin G showed interactions among α7-nAChR, Cav-1, cSRC, and Cx43 in rat cardiomyocytes. Immunoprecipitation with RyR2 (ryanodine receptor 2), SERCA2 9 sarcoplasmic/endoplasmic reticulum (Ca2+-ATPase), NCX1 (sodium-calcium exchange), cSRC, and normal rabbit immunoglobulin G exhibited interactions among RyR2, SERCA2, NCX1, and cSRC in rat cardiomyocytes. Normal rabbit immunoglobulin G was a negative control in these experiments.

The frozen sections of the rat heart were observed under a fluorescence microscope, and the eGFP (enhanced green fluorescent protein) tag exhibited green fluorescence, which means that the injection with AAVCav-1 or AAVCtrl was successful; the Western blotting showed that the infusion of $AAV^{Cav\text{-}1}$ increased the expression of Cav-1 and AAV^{Ctrl} did not (Figure 6B). Compared with the Sham group, the ICM group had fewer interactions between Cav-1 and α7-nAChR and cSRC; cSRC and Cav-1 and Cx43 (Figure 6C; ICM versus Sham, α7-nAChR/Cav-1 0.30±0.09 versus 1.39±0.10 *P*<0.001, cSRC/Cav-1 0.48±0.07 versus 0.76±0.06 *P*<0.001, Cx43/Cav-1 0.31±0.05 versus 0.77±0.06 *P*<0.001); the LIPUS improved these interactions (Figure 6C; ICM+LIPUS versus ICM, α7-nAChR/Cav-1 1.06±0.13 versus 0.30±0.09 *P*<0.001, cSRC/Cav-1 0.72±0.06 versus 0.48±0.07 *P*<0.001, Cx43/Cav-1 0.62±0.07 versus 0.31±0.05 *P*<0.001). Vagotomy suppressed the influence of LIPUS (Figure 6C; ICM+LIPUS+vagotomy versus ICM+LIPUS, α7-nAChR/Cav-1 0.37±0.07 versus 1.06±0.13 *P*<0.001, cSRC/Cav-1 0.44±0.06 versus 0.72±0.06 *P*<0.001, Cx43/Cav-1 0.33±0.05 versus 0.62±0.07 *P*<0.001). Cav-1 overexpression normalized those interactions partially (Figure 6C; ICM+LIPUS+vagotomy+$AAV^{Cav\text{-}1}$ versus ICM+LIPUS+vagotomy, α7-nAChR/Cav-1 1.22±0.13 versus 0.37±0.07 *P*<0.001, cSRC/Cav-1 0.71±0.08 versus 0.44±0.06 *P*=0.001, Cx43/Cav-1 0.68±0.08 versus 0.33±0.05 *P*<0.001). The Western blotting results in Figure 6D showed that vagotomy suppressed the positive influence of LIPUS among fibrosis, inflammation, and ion channel proteins, and Cav-1 overexpression reset the negative influences of vagotomy

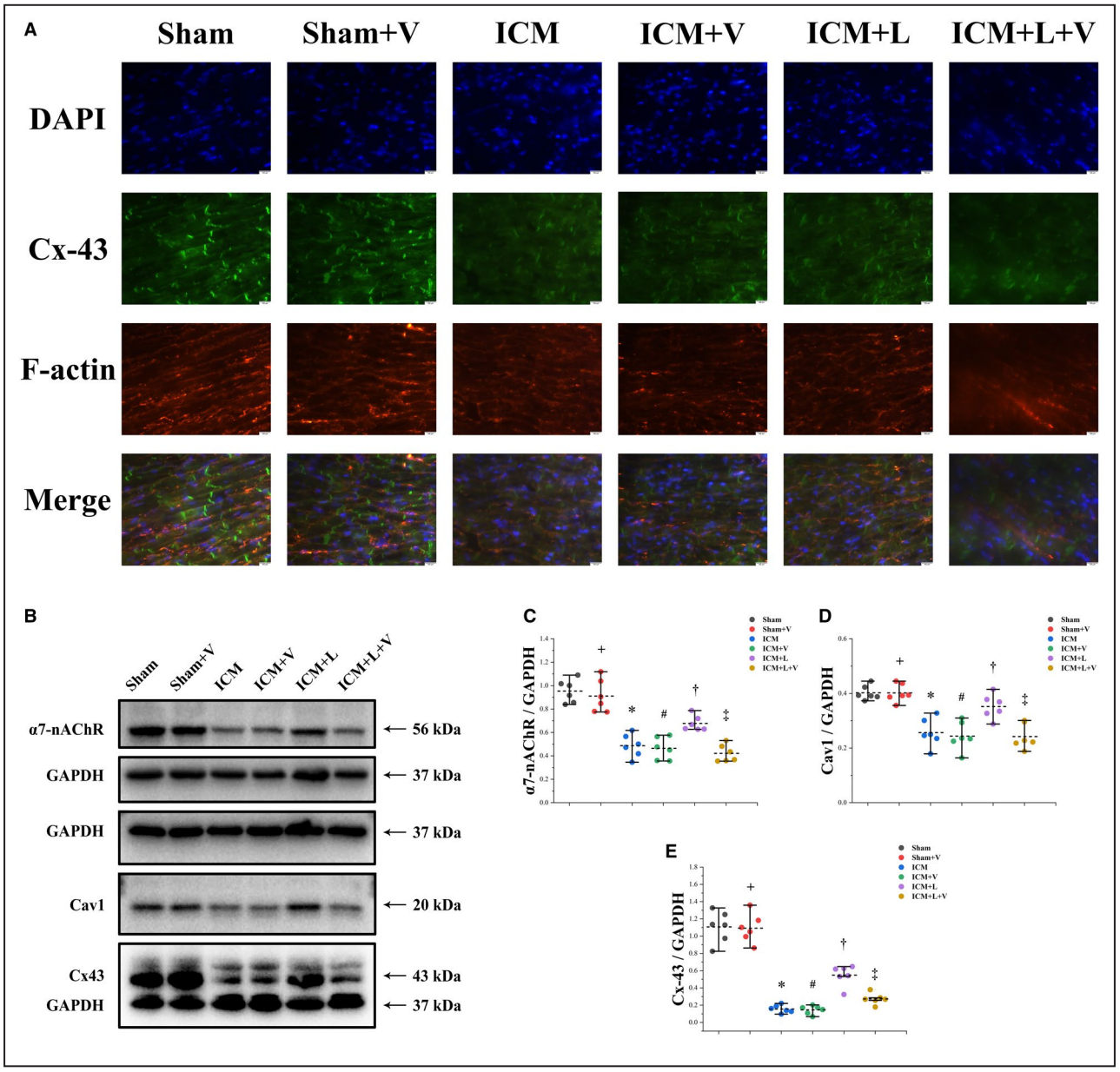

Figure 5. Effect of LIPUS on α7-nAChR, caveolin-1, and connexin-43 distribution.
A, Immunofluorescence images of protein Cx43 and F-actin from left ventricles of rats, n=6 of each group (magnification×200). The positive immuno-active signals of Cx43 (green) were accumulated in intercellular positions. The increased and nonuniform of F-Actin (red) represent cardiomyocyte hypertrophy and damage. The expression of protein Cx43 was significantly decreased in the ICM rats when compared with the Sham rats, and compared with the Sham group, F-actin was evidently increased and nonuniform in the ICM group. The intervention of LIPUS improved the expression of Cx43. Compared with ICM+L group, vagotomy downregulated the effect of LIPUS intervention. **B** through **D**, Results of Western blotting of Cx43, n=6 of each group. All data are expressed as the means±SD. **P*<0.05 compared with Sham group, †*P*<0.05 compared with ICM group, ‡*P*<0.05 compared with ICM+L group, +*P*>0.05 compared with Sham group, #*P*>0.05 compared with ICM group. The actual *P* values can be found in the Results. α7-nAChR indicates alpha-7 nicotinic receptor; Cav-1, caveolin-1; Cx43, connexin-43; ICM, ischemic cardiomyopathy; L, LIPUS group; LIPUS, low-intensity pulsed ultrasound; and V, vagotomy group.

partially (ICM+LIPUS+vagotomy+AAV$^{Cav\text{-}1}$ versus ICM+LIPUS+vagotomy, RyR2/GAPDH 0.97±0.23 versus 0.45±0.14 *P*=0.012, SERCA2/GAPDH 0.99±0.18 versus 0.45±0.11 *P*=0.002, NCX1/GAPDH 1.36±0.21 versus 0.55±0.10 *P*=0.001, collagen I/GAPDH 1.11±0.23 versus 2.07±0.32 *P*=0.002, collagen III/GAPDH 1.53±0.33 versus 2.47±0.53 *P*=0.046, IL-6/GAPDH 1.15±0.29 versus 2.01±0.48 *P*=0.043, TNF-α/GAPDH 1.08±0.24 versus 1.96±0.35 *P*=0.006, p-NF-κB p65/NF-κB p65 1.00±0.17 versus 2.02±0.31 *P*=0.001).

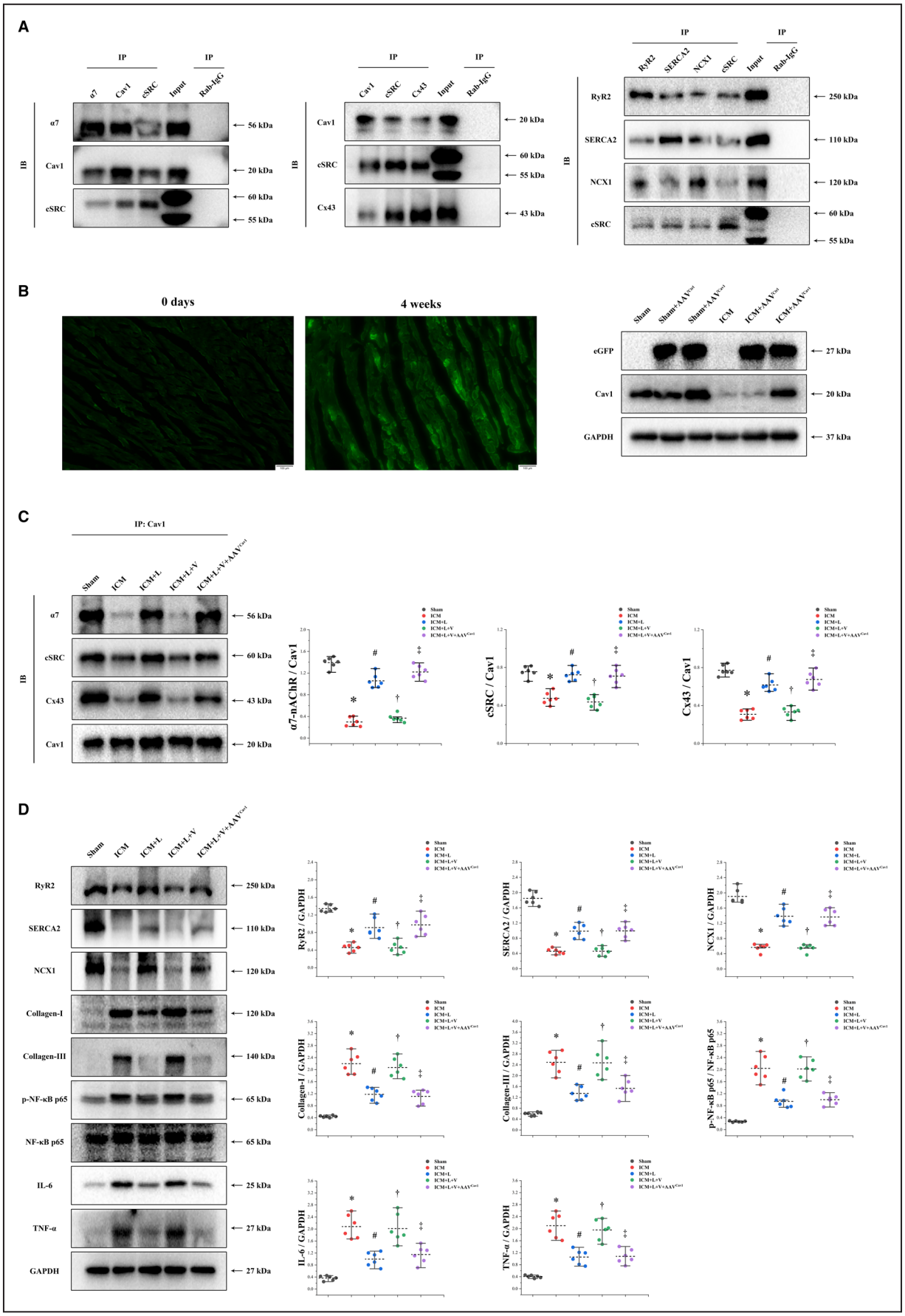
A
IP
IP
α7
Cav1
eSRC
Input
Rab-IgG
IB
α7
Cav1
eSRC
56 kDa
20 kDa
60 kDa
55 kDa
Cav1
cSRC
Cx43
Input
Rab-IgG
Cav1
cSRC
Cx43
20 kDa
60 kDa
55 kDa
43 kDa
RyR2
SERCA2
NCX1
cSRC
Input
Rab-IgG
RyR2
SERCA2
NCX1
cSRC
250 kDa
110 kDa
120 kDa
60 kDa
55 kDa
B
0 days
4 weeks
Sham
Sham+AAV^Cav1
Sham+AAV^Cav1
ICM
ICM+AAV^Cav1
ICM+AAV^Cav1
eGFP
Cav1
GAPDH
27 kDa
20 kDa
37 kDa
C
IP: Cav1
Sham
ICM
ICM+L
ICM+L+V
ICM+L+V+AAV^Cav1
α7
cSRC
Cx43
Cav1
56 kDa
60 kDa
43 kDa
20 kDa
α7-nAChR / Cav1
cSRC / Cav1
Cx43 / Cav1
D
Sham
ICM
ICM+L
ICM+L+V
ICM+L+V+AAV^Cav1
RyR2
SERCA2
NCX1
Collagen-I
Collagen-III
p-NF-κB p65
NF-κB p65
IL-6
TNF-α
GAPDH
250 kDa
110 kDa
120 kDa
120 kDa
140 kDa
65 kDa
65 kDa
25 kDa
27 kDa
27 kDa
RyR2 / GAPDH
SERCA2 / GAPDH
NCX1 / GAPDH
Collagen-I / GAPDH
Collagen-III / GAPDH
p-NF-κB p65 / NF-κB p65
IL-6 / GAPDH
TNF-α / GAPDH

Figure 6. Cav-1 overexpression reversed the negative influences of vagotomy on LIPUS.
A, Coimmunoprecipitation experiments of α7-nAChR, Cav-1, and cSRC; Cav-1, cSRC, and Cx43; and RyR2, SERCA2, NCX1, and cSRC in rat cardiomyocytes. All used normal rabbit immunoglobulin G as negative control. **B**, The eGFP tag was observed under fluorescence microscope and the Western blotting results of eGFP tag and Cav-1 (the groups were numbered sequentially as Sham, Sham+AAV^{Crtl}, Sham+AAV^{Cav-1}, ICM, ICM+ AAV^{Crtl}, ICM+ AAV^{Cav-1}). **C**, Compared with Sham rats, ICM rats had reduced associations of α7-nAChR/Cav-1, cSRC/Cav-1 and Cx43/Cav-1 (ICM vs Sham, P<0.05). LIPUS improved these interactions (ICM+L versus ICM, P<0.05), whereas the vagotomy suppressed them (ICM+L+V vs ICM+L, P<0.05), and Cav-1 overexpression normalized them (ICM+L+V+AAV^{Cav-1} vs ICM+L+V, P<0.05). **D**, The Western blotting and their analysis results (the groups were numbered sequentially as Sham, ICM, ICM+L, ICM+L+V, ICM+L+V+AAV^{Cav-1}). All n=6 of each group. All data are expressed as the means±SD. *P<0.05 compared with Sham group, #P<0.05 compared with ICM group, †P<0.05 compared with ICM+L group, ‡P<0.05 compared with ICM+L+V group. The actual P values can be found in the Results. α7-nAChR indicates alpha-7 nicotinic receptor; AAV, adeno-associated virus serotype 9; Cav-1, caveolin-1; Cx43, connexin-43; eGFP, enhanced green fluorescent protein; ICM, ischemic cardiomyopathy; IP, immunoprecipitation; L, LIPUS group; LIPUS, low-intensity pulsed ultrasound; NCX1, sodium-calcium exchange; RyR2, ryanodine receptor 2; SERCA2, sarcoplasmic/endoplasmic reticulum Ca2+-ATPase; and V, vagotomy group.

DISCUSSION

We found that LIPUS improves the cardiac function of ICM and shows positive cardiac electrophysiological changes in the ICM rats. Based on our explorations, we found that activation of the cholinergic anti-inflammatory pathway may be the key mechanism involved in the beneficial effects of LIPUS, and Cav-1 may play an essential role in its downstream.

Compared with the Sham group, the ICM group showed significantly lower cardiac ejection function and enlarged LVEDd and LVESd. The infarct border zone of the ICM rats performed higher fibrosis and remained chronically inflamed. Prolonged QTc and faulty cardiac autonomic function of ICM rats led to a higher risk of programmed electric stimulation-induced malignant arrhythmia. The myocardial sarcomeres contraction function of the ICM group and the expression of protein Cx43 in ICM rats were significantly decreased. LIPUS improved these harmful effects. Higher SS, SDV, SRV, SBP, diastolic blood pressure, LVSP, lower LVEDP, and shorter TTP RT indicated enhanced cardiac function. Vagotomy blunted the beneficial effects of LIPUS. We set the Sham+vagotomy and ICM+vagotomy groups to rule out the tachycardia effect by vagotomy. The results were not significantly different (Sham versus Sham+vagotomy, ICM versus ICM+vagotomy). To explain our results, the possible hypothesis is that the immune system becomes persistently active after the left anterior descending coronary artery infarction and causes the accumulation of cytokines in the injured site regionally, which influences angiogenesis, facilitates fibrosis, promotes autophagy, and causes myocardial edema and chronic inflammation.[12,13]

ICM is the end stage of ischemic heart disease; patients who survive MI will eventually progress to ICM, which will reduce the quality of life and life expectancy. These patients will suffer refractory heart failure and malignant arrhythmia.[14,15] The unique environment of the infarct border zone leads to a distinct pathological condition. The semi-ischemic environment results in semihypoxia and a lack of nutrients, which in turn causes aseptic chronic inflammation, chronic fibrosis, and ventricular remodeling. Numerous studies have shown that the pathological characteristics of postinfarct cardiomyocyte remodeling are associated with myocardial fibrosis, angiogenesis, autophagy, oxidative stress, and apoptosis. In these processes, persistent low-level inflammation plays a key role.[16,17] Modulation of the inflammation could postpone, and to some extent even reverse the process of the remodeling.[18] After infarction, most ventricular cardiomyocytes at the infarct and infarct border zone died. Surviving Purkinje fibers and newborn fibrous tissues perform prolonged action potentials and enhanced automaticity.[19] Ventricular remodeling led to cardiac electrophysiological changes, causing persistent abnormal electrical activity and impulse propagation, increasing the risk of malignant arrhythmia and sudden cardiac death, which had long been proven to be related to changes in the gap junction, especially the Cx43.[20,21] The functional preservation of Cx43 protein and the modulation of inflammation played an irreplaceable role in protection during ICM.[22] In our study, the protection effect of LIPUS in preserving Cx43 protein showed that LIPUS could improve cardiac autonomic function and reduce the risk of malignant arrhythmia. Vagotomy suppressed the effects of LIPUS.

Although medical technology has made significant progress, we still have limited options to improve the development and progression of heart failure and fatal ventricular arrhythmia induced by cardiac ischemia, which makes the clinical treatment of ICM a challenging problem. Currently, LIPUS is produced by a special ultrasound therapeutic apparatus. It is a noninvasive, gentle, and safe stimulation. This kind of stimulation is mechanically biased, which has been reported to activate the mechanotransduction system of various cells.[23] A series of research studies had proved that LIPUS could ameliorate inflammatory activity, such as in rheumatoid arthritis,[24] acute muscle tissue injury,[25] heart failure,[26] and viral myocarditis.[11]

We found that the ICM group exhibited high fibrosis, inflammation, and arrhythmia scores, with

programmed electric stimulation-induced malignant arrhythmia. LIPUS could significantly improve these harmful changes. The Western blotting results showed that LIPUS inhibited the activation of classic inflammatory signaling NF-κB after MI and reduced the release of proinflammatory cytokines such as TNF-α, IL-6, and IFN-γ (Figure 2B). In addition, the cholinergic anti-inflammatory pathway regulates the innate immune response to injury, pathogens, and tissue ischemia. It is the efferent, or motor arm of the inflammatory reflex, the neural circuit that responds to and regulates the inflammatory response.[27] Vagotomy suppressed these effects, which suggested that the cholinergic anti-inflammatory pathway was one of the underlying mechanisms of LIPUS.

On the other hand, heart failure of ICM decreases cardiac performance and rapidly affects multiple organ systems such as the neurohormonal systems, circulatory, and renal systems. Heart failure causes "energy starvation,"[28] which leads to chronic activation of the sympathetic nervous system and results in a maladaptive attempt to improve cardiac function.[29] The sarcomere contraction measurement experiment showed that the ICM rats had significantly lower SS, SDV, SRV, and longer TTP and RT than the Sham rats. It matched the cardiac ejection function measured by echocardiography, and LIPUS improved these indicators (Figure 4).

Furthermore, vaveolae play a role in mechanosensation in response to different mechanical stimuli such as stretching. Caveolae can sense, transduce, and buffer changing biomechanical perturbations.[30,31] Researchers found that Cav-1 was vital in cardioprotection under myocardial ischemia. Gap junctions, especially Cx43, were essential clusters of transmembrane channels whose downregulation and uncoupling were associated with a high risk of myocardial infarction-induced fatal ventricular arrhythmias.[32,33] Caveolar microdomains are abundant in cardiovascular system cells, including endothelial cells, cardiac fibroblasts, and cardiomyocytes. Interestingly, although Cav-1 is primarily expressed in endothelial cells of the heart, it has also been reported to be located on the myocardial cell membrane and perform physiological functions.[34] Evidence suggested that TGFβ (transforming growth factor beta) and TGFβ-related pathways were molecular mediators of cardiac fibrosis.[35] Cav-1 could regulate TGF-β1/Smad2 activity during cardiac injury and repair.[36] Other studies have indicated that Cav-1 is involved in the regulation of ion channels, which results in alterations to cardiac electrical function.[37] Alterations in Ca^{2+} homeostasis were responsible for excitation-contraction coupling defects and malignant arrhythmias.[38] Aberrant RyR opening in diastole and blunted SERCA2 (related to RyR2 complex) activity resulted in the abnormal occurrence of Ca^{2+} sparks.[39,40]

The coimmunoprecipitation results suggested that there was interaction between Cav-1 and α7-nAChR and Cx43 and Ca^{2+}-handling protein (SERCA2, RyR2, and NCX1), and cSRC may play a vital role between these interactions (Figure 6). Overexpression of Cav-1 normalized Ca^{2+}-handling protein levels by modulating phosphorylation-activation of cSRC to improve Ca^{2+} cycling.[41] Yang et al reported that the interaction between cSRC and Cav-1 modulated Cx43 gap junction homeostasis, affecting cardiac electrical activity under the renin-angiotensin-system-activated condition.[42] We discovered that α7-nAChR and Cav-1 expression was reduced in the infarct border zone of the ICM model, and LIPUS upregulated their expression, whereas vagotomy mitigated the effects of LIPUS (Figure 5). Then, we directly intervened with Cav-1 by heart-specific overexpression of Cav-1 and found that overexpression of Cav-1 partially reversed the effects of vagotomy (Figure 6).

CONCLUSIONS

We found that LIPUS directly affected regional anti-inflammation and antifibrosis, improved cardiac autonomic function and heart failure, protected the Cx43 protein, and reduced the risk of malignant arrhythmia at ICM. The cholinergic anti-inflammatory pathway was the essential mechanism involved, and Cav-1 may play an important role downstream. Our study provided a new, promising, noninvasive ICM treatment strategy.

ARTICLE INFORMATION

Received June 28, 2024; accepted January 6, 2025.

Affiliations

Department of Cardiology, The Second Affiliated Hospital and Yuying Children's Hospital of Wenzhou Medical University, Wenzhou, Zhejiang, China (Z-H.L., Q-L.Y., B-H.Y., W-C.X., H-L.H., K-Y.H., C.Z., S-J.W., J-F.L.); Key Laboratory of Panvascular Diseases of Wenzhou, Wenzhou, Zhejiang, China (Z-H.L., Q-L.Y., B-H.Y., W-C.X., H-L.H., K-Y.H., C.Z., S-J.W., J-F.L.); and Wenzhou Medical University, Wenzhou, China (Z-H.L., Q-L.Y., B-H.Y., W-C.X., H-L.H., K-Y.H., C.Z., S-J.W., J-F.L.).

Acknowledgments

We appreciate the helpful comments on this paper received from our editors and reviewers.

Sources of Funding

Research was supported by Grant No. 82300351 and No. 82070333 from the National Natural Science Foundation of China, grant No. LY21H020011 from the Zhejiang Provincial Natural Science Foundation of China, and Grant No. ZY2020018 from the Wenzhou Science and Technology Bureau Major Scientific Research Project.

Disclosures

None.

Supplemental Material

Data S1
Table S1
Figures S1–S2
References 43–53

REFERENCES

1. Global, regional, and national age-sex-specific mortality for 282 causes of death in 195 countries and territories, 1980–2017: a systematic analysis for the Global Burden of Disease study 2017. *Lancet*. 2018;392:1736–1788. doi: 10.1016/s0140-6736(18)32203-7
2. *Mid-Point Evaluation of the Implementation of the WHO Global Action Plan for the Prevention and Control of Noncommunicable Diseases 2013–2020 (NCD-GAP): Management Response*. World Health Organization; 2022. https://www.who.int/publications/m/item/mid-point-evaluation-of-the-implementation-of-the-who-global-action-plan-for-the-prevention-and-control-of-noncommunicable-diseases-2013-2020-(ncd-gap)---management-response
3. Liu S, Zhou M, Li J, Hu B, Jiang D, Huang H, Song J. LIPUS inhibited the expression of inflammatory factors and promoted the osteogenic differentiation capacity of hPDLCs by inhibiting the NF-κB signaling pathway. *J Periodontal Res*. 2020;55:125–140. doi: 10.1111/jre.12696
4. Lynn JG, Zwemer RL, Chick AJ. The biological application of focused ultrasonic waves. *Science*. 1942;96:119–120. doi: 10.1126/science.96.2483.119
5. Rubin C, Bolander M, Ryaby JP, Hadjiargyrou M. The use of low-intensity ultrasound to accelerate the healing of fractures. *J Bone Joint Surg Am*. 2001;83:259–270. doi: 10.2106/00004623-200102000-00015
6. Erdogan O, Esen E, Ustün Y, Kürkçü M, Akova T, Gönlüşen G, Uysal H, Cevlik F. Effects of low-intensity pulsed ultrasound on healing of mandibular fractures: an experimental study in rabbits. *J Oral Maxillofac Surg*. 2006;64:180–188. doi: 10.1016/j.joms.2005.10.027
7. Liu B, Chen W, Jiang J, Zhou W, Zhang Y, He R, Wang Y, Li J, Liang D, Chen J, et al. Treatment effect of low-intensity pulsed ultrasound on benzene- and cyclophosphamide-induced aplastic anemia in rabbits. *Phys Ther*. 2019;99:1443–1452. doi: 10.1093/ptj/pzz074
8. Li XH, Guo D, Chen LQ, Chang ZH, Shi JX, Hu N, Chen C, Zhang XW, Bao SQ, Chen MM, et al. Low-intensity ultrasound ameliorates brain organoid integration and rescues microcephaly deficits. *Brain*. 2024;147:3817–3833. doi: 10.1093/brain/awae150
9. Eguchi K, Shindo T, Ito K, Ogata T, Kurosawa R, Kagaya Y, Monma Y, Ichijo S, Kasukabe S, Miyata S, et al. Whole-brain low-intensity pulsed ultrasound therapy markedly improves cognitive dysfunctions in mouse models of dementia—crucial roles of endothelial nitric oxide synthase. *Brain Stimul*. 2018;11:959–973. doi: 10.1016/j.brs.2018.05.012
10. Shindo T, Ito K, Ogata T, Hatanaka K, Kurosawa R, Eguchi K, Kagaya Y, Hanawa K, Aizawa K, Shiroto T, et al. Low-intensity pulsed ultrasound enhances angiogenesis and ameliorates left ventricular dysfunction in a mouse model of acute myocardial infarction. *Arterioscler Thromb Vasc Biol*. 2016;36:1220–1229. doi: 10.1161/atvbaha.115.306477
11. Zheng C, Wu SM, Lian H, Lin YZ, Zhuang R, Thapa S, Chen QZ, Chen YF, Lin JF. Low-intensity pulsed ultrasound attenuates cardiac inflammation of CVB3-induced viral myocarditis via regulation of caveolin-1 and MAPK pathways. *J Cell Mol Med*. 2019;23:1963–1975. doi: 10.1111/jcmm.14098
12. Brakenhielm E, Alitalo K. Cardiac lymphatics in health and disease. *Nat Rev Cardiol*. 2019;16:56–68. doi: 10.1038/s41569-018-0087-8
13. Lafuse WP, Wozniak DJ, Rajaram MVS. Role of cardiac macrophages on cardiac inflammation, fibrosis and tissue repair. *Cells*. 2020;10:51. doi: 10.3390/cells10010051
14. Cabac-Pogorevici I, Muk B, Rustamova Y, Kalogeropoulos A, Tzeis S, Vardas P. Ischaemic cardiomyopathy. Pathophysiological insights, diagnostic management and the roles of revascularisation and device treatment. Gaps and dilemmas in the era of advanced technology. *Eur J Heart Fail*. 2020;22:789–799. doi: 10.1002/ejhf.1747
15. Zweck E, Thayer KL, Helgestad OKL, Kanwar M, Ayouty M, Garan AR, Hernandez-Montfort J, Mahr C, Wencker D, Sinha SS, et al. Phenotyping cardiogenic shock. *J Am Heart Assoc*. 2021;10:e020085. doi: 10.1161/jaha.120.020085
16. Horckmans M, Bianchini M, Santovito D, Megens RTA, Springael JY, Negri I, Vacca M, Di Eusanio M, Moschetta A, Weber C, et al. Pericardial adipose tissue regulates granulopoiesis, fibrosis, and cardiac function after myocardial infarction. *Circulation*. 2018;137:948–960. doi: 10.1161/circulationaha.117.028833
17. Zhang Q, Wang L, Wang S, Cheng H, Xu L, Pei G, Wang Y, Fu C, Jiang Y, He C, et al. Signaling pathways and targeted therapy for myocardial infarction. *Signal Transduct Target Ther*. 2022;7:78. doi: 10.1038/s41392-022-00925-z
18. Marinković G, Koenis DS, de Camp L, Jablonowski R, Graber N, de Waard V, de Vries CJ, Goncalves I, Nilsson J, Jovinge S, et al. S100A9 links inflammation and repair in myocardial infarction. *Circ Res*. 2020;127:664–676. doi: 10.1161/circresaha.120.315865
19. Lubberding AF, Sattler SM, Flethøj M, Tfelt-Hansen J, Jespersen T. Comparison of hemodynamics, cardiac electrophysiology, and ventricular arrhythmia in an open- and a closed-chest porcine model of acute myocardial infarction. *Am J Physiol Heart Circ Physiol*. 2020;318:H391–h400. doi: 10.1152/ajpheart.00406.2019
20. Matsushita T, Takamatsu T. Ischaemia-induced temporal expression of connexin43 in rat heart. *Virchows Arch*. 1997;431:453–458. doi: 10.1007/s004280050123
21. Yao JA, Gutstein DE, Liu F, Fishman GI, Wit AL. Cell coupling between ventricular myocyte pairs from connexin43-deficient murine hearts. *Circ Res*. 2003;93:736–743. doi: 10.1161/01.Res.0000095977.66660.86
22. Chowdhury RA, Debney MT, Protti A, Handa BS, Patel KHK, Lyon AR, Shah AM, Ng FS, Peters NS. Rotigaptide infusion for the first 7 days after myocardial infarction-reperfusion reduced late complexity of myocardial architecture of the healing border-zone and arrhythmia inducibility. *J Am Heart Assoc*. 2021;10:e020006. doi: 10.1161/jaha.120.020006
23. Izadifar Z, Babyn P, Chapman D. Mechanical and biological effects of ultrasound: a review of present knowledge. *Ultrasound Med Biol*. 2017;43:1085–1104. doi: 10.1016/j.ultrasmedbio.2017.01.023
24. Nakamura T, Fujihara S, Yamamoto-Nagata K, Katsura T, Inubushi T, Tanaka E. Low-intensity pulsed ultrasound reduces the inflammatory activity of synovitis. *Ann Biomed Eng*. 2011;39:2964–2971. doi: 10.1007/s10439-011-0408-0
25. da Silva Junior EM, Mesquita-Ferrari RA, França CM, Andreo L, Bussadori SK, Fernandes KPS. Modulating effect of low intensity pulsed ultrasound on the phenotype of inflammatory cells. *Biomed Pharmacother*. 2017;96:1147–1153. doi: 10.1016/j.biopha.2017.11.108
26. Ogata T, Ito K, Shindo T, Hatanaka K, Eguchi K, Kurosawa R, Kagaya Y, Monma Y, Ichijo S, Taki H, et al. Low-intensity pulsed ultrasound enhances angiogenesis and ameliorates contractile dysfunction of pressure-overloaded heart in mice. *PLoS One*. 2017;12:e0185555. doi: 10.1371/journal.pone.0185555
27. Rosas-Ballina M, Ochani M, Parrish WR, Ochani K, Harris YT, Huston JM, Chavan S, Tracey KJ. Splenic nerve is required for cholinergic antiinflammatory pathway control of TNF in endotoxemia. *Proc Natl Acad Sci USA*. 2008;105:11008–11013. doi: 10.1073/pnas.0803237105
28. Ingwall JS. On the hypothesis that the failing heart is energy starved: lessons learned from the metabolism of ATP and creatine. *Curr Hypertens Rep*. 2006;8:457–464. doi: 10.1007/s11906-006-0023-x
29. Marks AR. Calcium cycling proteins and heart failure: mechanisms and therapeutics. *J Clin Invest*. 2013;123:46–52. doi: 10.1172/jci62834
30. Chai Q, Wang XL, Zeldin DC, Lee HC. Role of caveolae in shear stress-mediated endothelium-dependent dilation in coronary arteries. *Cardiovasc Res*. 2013;100:151–159. doi: 10.1093/cvr/cvt157
31. Cheng JP, Mendoza-Topaz C, Howard G, Chadwick J, Shvets E, Cowburn AS, Dunmore BJ, Crosby A, Morrell NW, Nichols BJ. Caveolae protect endothelial cells from membrane rupture during increased cardiac output. *J Cell Biol*. 2015;211:53–61. doi: 10.1083/jcb.201504042
32. Greener ID, Sasano T, Wan X, Igarashi T, Strom M, Rosenbaum DS, Donahue JK. Connexin43 gene transfer reduces ventricular tachycardia susceptibility after myocardial infarction. *J Am Coll Cardiol*. 2012;60:1103–1110. doi: 10.1016/j.jacc.2012.04.042
33. Patel HH, Tsutsumi YM, Head BP, Niesman IR, Jennings M, Horikawa Y, Huang D, Moreno AL, Patel PM, Insel PA, et al. Mechanisms of cardiac protection from ischemia/reperfusion injury: a role for caveolae and caveolin-1. *FASEB J*. 2007;21:1565–1574. doi: 10.1096/fj.06-7719com
34. Cho WJ, Chow AK, Schulz R, Daniel EE. Caveolin-1 exists and may function in cardiomyocytes. *Can J Physiol Pharmacol*. 2010;88:73–76. doi: 10.1139/y09-114
35. Miyasato SK, Loeffler J, Shohet R, Zhang J, Lindsey M, Le Saux CJ. Caveolin-1 modulates TGF-β1 signaling in cardiac remodeling. *Matrix Biol*. 2011;30:318–329. doi: 10.1016/j.matbio.2011.05.003
36. Khalil H, Kanisicak O, Prasad V, Correll RN, Fu X, Schips T, Vagnozzi RJ, Liu R, Huynh T, Lee SJ, et al. Fibroblast-specific TGF-β-Smad2/3 signaling underlies cardiac fibrosis. *J Clin Invest*. 2017;127:3770–3783. doi: 10.1172/jci94753
37. Darby PJ, Kwan CY, Daniel EE. Caveolae from canine airway smooth muscle contain the necessary components for a role in Ca 2+ handling. *Am J Physiol Lung Cell Mol Physiol*. 2000;279:L1226–L1235. doi: 10.1152/ajplung.2000.279.6.L1226

38. Ikeda Y, Hoshijima M, Chien KR. Toward biologically targeted therapy of calcium cycling defects in heart failure. *Physiology (Bethesda)*. 2008;23:6–16. doi: 10.1152/physiol.00033.2007
39. Fauconnier J, Thireau J, Reiken S, Cassan C, Richard S, Matecki S, Marks AR, Lacampagne A. Leaky RyR2 trigger ventricular arrhythmias in Duchenne muscular dystrophy. *Proc Natl Acad Sci USA*. 2010;107:1559–1564. doi: 10.1073/pnas.0908540107
40. Thireau J, Karam S, Roberge S, Roussel J, Aimond F, Cassan C, Gac A, Babuty D, Le Guennec JY, Lacampagne A, et al. B-adrenergic blockade combined with subcutaneous B-type natriuretic peptide: a promising approach to reduce ventricular arrhythmia in heart failure? *Heart*. 2014;100:833–841. doi: 10.1136/heartjnl-2013-305167
41. Wu SJ, He RL, Zhao L, Yu XY, Jiang YN, Guan X, Chen QY, Ren FF, Xie ZY, Wu LP, et al. Cardiac-specific overexpression of caveolin-1 in rats with ischemic cardiomyopathy improves arrhythmogenicity and cardiac remodelling. *Can J Cardiol*. 2023;39:73–86. doi: 10.1016/j.cjca.2022.10.005
42. Yang KC, Rutledge CA, Mao M, Bakhshi FR, Xie A, Liu H, Bonini MG, Patel HH, Minshall RD, Dudley SC Jr. Caveolin-1 modulates cardiac gap junction homeostasis and arrhythmogenecity by regulating cSrc tyrosine kinase. *Circ Arrhythm Electrophysiol*. 2014;7:701–710. doi: 10.1161/circep.113.001394
43. Percie du Sert N, Hurst V, Ahluwalia A, Alam S, Avey MT, Baker M, Browne WJ, Clark A, Cuthill IC, Dirnagl U, et al. The ARRIVE guidelines 2.0: updated guidelines for reporting animal research. *PLoS Biol*. 2020;18:e3000410. doi: 10.1371/journal.pbio.3000410
44. Jayasankar V, Woo YJ, Bish LT, Pirolli TJ, Berry MF, Burdick J, Bhalla RC, Sharma RV, Gardner TJ, Sweeney HL. Inhibition of matrix metalloproteinase activity by TIMP-1 gene transfer effectively treats ischemic cardiomyopathy. *Circulation*. 2004;110:Ii180–Ii186. doi: 10.1161/01.Cir.0000138946.29375.49
45. Felker GM, Shaw LK, O'Connor CM. A standardized definition of ischemic cardiomyopathy for use in clinical research. *J Am Coll Cardiol*. 2002;39:210–218. doi: 10.1016/s0735-1097(01)01738-7
46. Nishina T, Nishimura K, Yuasa S, Miwa S, Nomoto T, Sakakibara Y, Handa N, Hamanaka I, Saito Y, Komeda M. Initial effects of the left ventricular repair by plication may not last long in a rat ischemic cardiomyopathy model. *Circulation*. 2001;104:I241–I245. doi: 10.1161/hc37t1.094522
47. Hou Z, Qin X, Hu Y, Zhang X, Li G, Wu J, Li J, Sha J, Chen J, Xia J, et al. Longterm exercise-derived exosomal miR-342-5p: a novel exerkine for cardioprotection. *Circ Res*. 2019;124:1386–1400. doi: 10.1161/circresaha.118.314635
48. Nguyen T, El Salibi E, Rouleau JL. Postinfarction survival and inducibility of ventricular arrhythmias in the spontaneously hypertensive rat: effects of ramipril and hydralazine. *Circulation*. 1998;98:2074–2080. doi: 10.1161/01.cir.98.19.2074
49. Harrison A, Lin S, Pounder N, Mikuni-Takagaki Y. Mode & mechanism of low intensity pulsed ultrasound (LIPUS) in fracture repair. *Ultrasonics*. 2016;70:45–52. doi: 10.1016/j.ultras.2016.03.016
50. Henze M, Tiniakov R, Samarel A, Holmes E, Scrogin K. Chronic fluoxetine reduces autonomic control of cardiac rhythms in rats with congestive heart failure. *Am J Physiol Heart Circ Physiol*. 2013;304:H444–H454. doi: 10.1152/ajpheart.00763.2012
51. Bélichard P, Savard P, Cardinal R, Nadeau R, Gosselin H, Paradis P, Rouleau JL. Markedly different effects on ventricular remodeling result in a decrease in inducibility of ventricular arrhythmias. *J Am Coll Cardiol*. 1994;23:505–513. doi: 10.1016/0735-1097(94)90440-5
52. Yu J, Zhang HF, Wu F, Li QX, Ma H, Guo WY, Wang HC, Gao F. Insulin improves cardiomyocyte contractile function through enhancement of SERCA2a activity in simulated ischemia/reperfusion. *Acta Pharmacol Sin*. 2006;27:919–926. doi: 10.1111/j.1745-7254.2006.00388.x
53. Ren J, Wold LE. Measurement of cardiac mechanical function in isolated ventricular myocytes from rats and mice by computerized video-based imaging. *Biol Proced Online*. 2001;3:43–53. doi: 10.1251/bpo22